


# Image Cover Sheet

96-03522

<b>CLASSIFICATION</b>  UNCLASSIFIED	<b>SYSTEM NUMBER</b> 500040 
---	--

**TITLE**  
ATMOSPHERIC REMOTE SENSING WITH A GROUND-BASED SPECTROMETER SYSTEM.

**System Number:**  
**Patron Number:**  
**Requester:**

**Notes:**

**DSIS Use only:**  
**Deliver to:** FF



# PROCEEDINGS REPRINT



SPIE—The International Society for Optical Engineering

*Reprinted from*

## *Infrared Technology and Applications XXII*

8–12 April 1996  
Orlando, Florida



**Volume 2744**

## Atmospheric Remote Sensing with a Ground-based Spectrometer System

J.-M. Thériault, C. Bradette and J. Gilbert\*

DREV-Defence Research Establishment Valcartier  
P.O. Box 8800, Québec, Canada, G0A 1R0

\* INFORMISSION - Ste Foy, Québec, Canada G1N 4N6

### ABSTRACT

Recent developments in atmospheric monitoring with a ground-based FTIR spectrometer are presented. Several aspects of the inversion method for the retrieval of temperature and humidity profiles from IR emission spectra are reported. The potential of the remote sensing method is analyzed in the context of three specific applications: As an aid for predictions of atmospheric transmittances, in support to the remote detection of atmospheric pollutants (CFCs) and to the evaluation of cloud parameters.

Keywords: remote sensing, Fourier spectrometer, atmospheric radiance, temperature profile, humidity profile

### 1. INTRODUCTION

The potential of ground-based Fourier transform IR spectrometer (FTIR) for probing the downwelling radiance of the atmosphere has been proposed or exploited in a number of recent applications such as for example, boundary layer and tropospheric profiling<sup>1-2</sup>, urban pollution studies<sup>3</sup> and CFCs thermal emission monitoring<sup>4</sup>. In order to develop a method for the retrieval of temperature and water vapor profiles from IR emission spectra, the Defence Research Establishment Valcartier (DREV) has acquired a device referred to as the Double input Beam Interferometer Sounder (DBIS)<sup>2</sup>. Since summer 1992, the DBIS has been deployed in a series of field experiments, producing spectral data of good quality for a variety of sky conditions. These spectral data are now being utilized as a guide in the development of our inversion method for temperature and humidity profile retrievals and also for several related applications..

In this paper, a general description of the remote sensing method is presented. The method is proposed and analyzed as a possible substitute to radiosondes in the context of three specific applications. First, the method is evaluated as an aid for predicting slant path transmittances. The potential of this approach is verified through several MODTRAN2 calculations performed to compare transmittances generated with radiosonde profiles ("exact") and retrieved profiles (approximate). Second, the remote detection of pollutants by FTIR emission spectroscopy usually requires that the background atmospheric contribution (clean atmosphere) be subtracted from measurement (polluted atmosphere) leading to a background free signature (residual) from which mixing ratios can be estimated. An analysis is performed to evaluate the accuracy of computing spectral residuals based on retrieved profiles rather than radiosonde profiles. Finally, ground based observations of cloud emissions in the IR has lead us to investigate a simple method for estimating the transmittance (at 9.3  $\mu\text{m}$ ) and the apparent temperature of clouds. The method takes advantage of the cloud extinction effects on the ozone emission near 9.6 micron.

### 2. SPECTRAL MEASUREMENT AND INVERSION

The DBIS consists of one or optionally two 10-in. diameter Cassegrain telescopes, optically coupled to a double-input port Fourier transform interferometer. The interferometer is a BOMEM model MB100 and has two detection units, one with an InSb detector and the other with a MCT detector. This configuration allows measurements of calibrated spectra according to the following specifications: 0-180° zenith angle, 5 mrad field of view, 3 to 20  $\mu\text{m}$  spectral band at 1  $\text{cm}^{-1}$  resolution. The pointing capability and small field of view of the instrument ensure a good radiometric homogeneity of the probed scene at large zenith angle (Z. A.).

Examples of downwelling emission spectra (Z.A.= 30 degree) expressed in radiance units appear in Fig. 1. Figure 1a corresponds to a typical clear sky radiance recorded in midlatitude summer conditions. The general shape of this spectrum is dominated by the temperature and the absorption properties of the constituents along the optical path. In spectral regions where the absorption is strong, the atmosphere radiates its energy like a blackbody at a temperature roughly equal

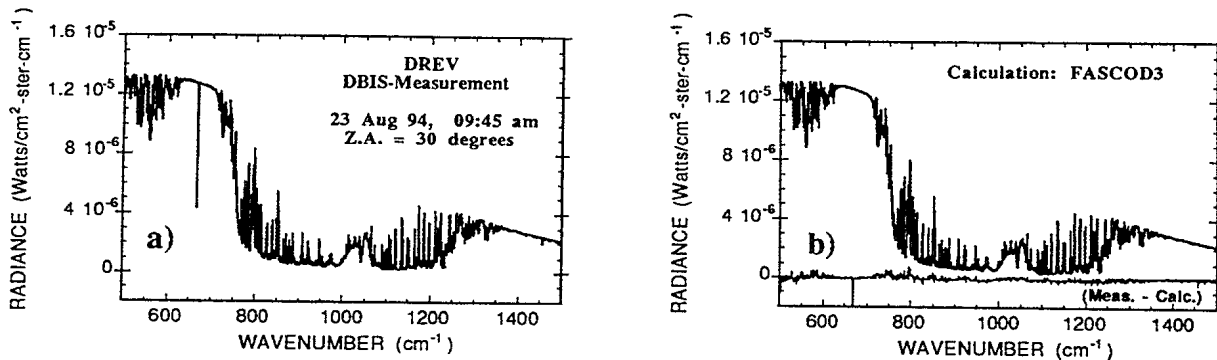


Figure 1: Typical ground-based measurement (a) of the downwelling spectral radiance compared to calculation (b) performed with radiosonde temperature and humidity profiles: Bottom curve represents the difference between measurement and calculation.

to the temperature near the sounder. This is observed in the strong absorption band of  $\text{CO}_2$  near  $15 \mu\text{m}$  ( $660 \text{ cm}^{-1}$ ) and also in the  $1300\text{-}1400 \text{ cm}^{-1}$  region ( $6.3 \mu\text{m}$ ) where the absorption is mainly due to water vapor. If we exclude the important emission band of the  $\text{O}_3$  near  $9.6 \mu\text{m}$  ( $1040 \text{ cm}^{-1}$ ), the atmospheric window region from  $800$  to  $1200 \text{ cm}^{-1}$  is dominated by the water vapor absorption lines (fine spectral structure) and continuum (smooth spectral shape). For comparison, the upper curve of Fig. 1b represents the corresponding calculation performed with a version of the FASCOD3 model<sup>5</sup>. The bottom curve of the Figure is the spectral residual defined as the difference between measured and calculated radiances.

The adopted approach for the retrieval of temperature and humidity profiles from radiance spectra is a minimum information type of inversion<sup>2,6</sup>. The formulation of this method can be summarized as follows. First, the forward problem of radiative transfer is linearized by considering that the measured radiance  $R(\nu)$  is a first order perturbation of the radiance  $R^0(\nu)$  computed with first guess profiles of temperature  $T^0(z)$  and water vapor mixing ratio  $\rho^0(z)$ . In its matrix form, the linearized radiative transfer equation is written as

$$r = K x \quad (1)$$

In eq. 1,  $r$  is the perturbation vector of spectral measurements defined as  $r = R(\nu) - R^0(\nu)$  and  $K$  is the matrix of partial derivatives where the rows of  $K$  are often defined as the weighting functions. The column vector  $x$  contains the perturbation profiles of temperature and mixing ratio. It is defined as  $x = [T(z) - T^0(z); \rho^0(z) - \rho^0(z)]$ . The minimum information solution of this overdetermined system of equations which contains about 1000 spectral elements for about 50 unknowns (30 levels for temperature and 20 levels for mixing ratio) is given by

$$x = [K^t S_e^{-1} K + S_b^{-1}]^{-1} K^t S_e^{-1} r \quad (2)$$

where  $S_e$  is a diagonal matrix having for elements the noise standard deviation associated with the spectral measurements and  $S_b$  is a diagonal matrix composed of damping parameters adjusted for each variable to be retrieved. These damping parameters are introduced to stabilize the solution which oscillates when improperly adjusted. Because of the linearization constraints in the problem, eq. 2 provides an approximate solution for the actual profiles. An improved solution might be obtained by iterations for which the  $K$  matrix is updated with the previous profile estimates.

The current inversion algorithm used in the present work is based on the FASCOD3 model and includes the Moncet scheme for partial derivative calculations. This scheme<sup>7</sup> greatly optimizes calculations of partial derivatives based on FASCODE. In addition, we have developed a systematic procedure<sup>8</sup> for the evaluation of first guess profiles required as input by the method. For water vapor, the first guess profile is given by an arithmetic average of midlatitude summer and

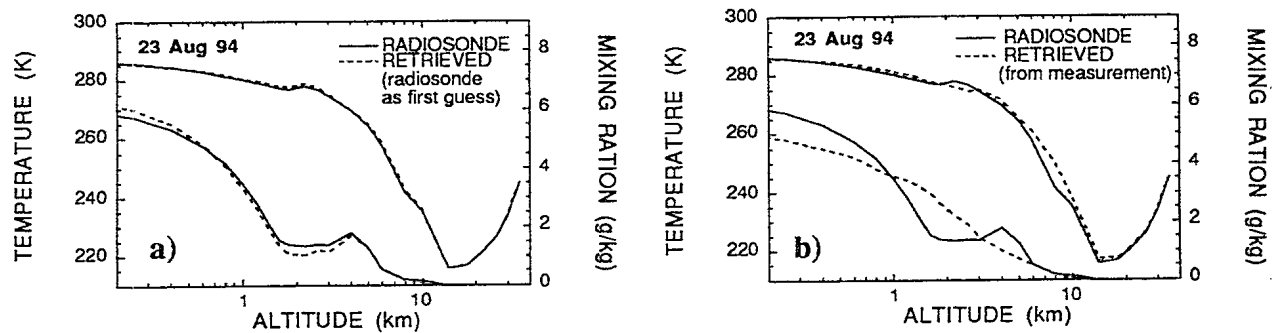


Figure 2: Typical inversions for spectral measurements performed with the DBIS. Case a, corresponds to the inversion of an experimental spectrum done with radiosonde data as first guess while for case b, the first guess is roughly estimated from specific channels of the radiance spectrum.

US standard profile, scaled with the measured radiance in a narrow band of  $\text{H}_2\text{O}$  near  $560\text{ cm}^{-1}$ . For temperature, the first guess profiles is given by an interpolation from profiles estimated near the surface ( $< 0.5\text{ km}$ ) and above  $8\text{ km}$  (assumed to be midlatitude summer). The near surface profile below  $0.5\text{ km}$  is evaluated from the measured radiance in the strong absorption band of  $\text{CO}_2$  near  $15\text{ }\mu\text{m}$ .

Figure 2 gives a typical example of results obtained with the actual inversion algorithm<sup>9</sup>. Figure 2a corresponds to the inversion of an experimental spectrum done with the radiosonde data taken as first guess: the radiosonde profiles of temperature and humidity are compared to retrieved profiles. Although the overall agreement is good there are slight differences that might be due to the fact that radiosonde and DBIS measurements were not perfectly coincident in time and direction. Figure 2b represents the desired results where the whole inversion process has been applied to the experimental spectrum. In this case, the first guess profiles is derived using the systematic procedure which requires only data from the measured spectrum itself. The agreement between radiosonde and retrieved profiles is acceptable but limited by the resulting vertical resolution especially for water vapor mixing ratios. These inversions represent what can be obtained with the minimum information type inversion in its present form. Potential improvements might be realized by a better selection of spectral bands, inclusion of missing species in the forward calculations and possibly a better evaluation of the reference blackbody emissivities.

### 3. TRANSMITTANCE PREDICTIONS BASED ON RETRIEVED PROFILES

The use of remote sensing as an aid for predicting slant path transmittances is a valuable approach to assess the performance of EO systems in real atmospheric conditions. As for other methods, the retrieval of temperature and water vapor profiles with the minimum information type inversion has its advantages and limitations. As a first step in evaluating the potential of our inversion method to provide inputs for transmittance predictions, a series of MODTRAN<sup>210</sup> calculations has been performed using retrieved profiles and radiosonde profiles<sup>8</sup>. The main objective is to estimate the transmittance errors introduced by the use of real retrieved profiles rather than the "exact" radiosonde data.

Figure 3 shows an example of slant path transmittance calculations in the IR for a zenith angle of  $80^\circ$  (space to ground) corresponding to atmospheric profiles recorded on 20 June 94 at DREV. For these calculations, the background atmosphere is given by the midlatitude summer model without aerosols. In Fig. 3, the full line corresponds to the "exact" transmittance computed with the radiosonde inputs, the dashed line represents the approximate transmittance computed with retrieved profiles and the bottom curves indicates the difference between the two. Because the difference is mainly due to water vapor, the agreement is much better in the mid IR ( $2000\text{-}3000\text{ cm}^{-1}$ ) with typical error of approximately 1 % while in the far IR ( $800\text{-}1200\text{ cm}^{-1}$ ) the error reach a maximum of 4 % near  $12\text{ }\mu\text{m}$ . Calculations have been done for several zenith angles of  $0^\circ$ ,  $45^\circ$ ,  $80^\circ$  and optical path lengths of 2, 10 and 30 km. The overall agreement is rather good in all cases meaning that the retrieved profiles would have introduced at worst an error smaller than 5 %.

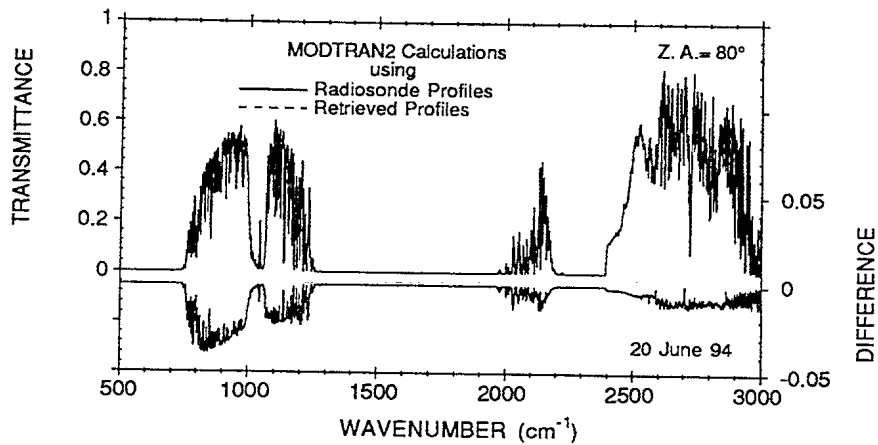


Figure 3: a) Slant path transmittance (space to ground) predictions based on radiosonde and retrieved profiles for a zenith angle of  $80^\circ$ . The bottom curve is the difference between them (right scale).

#### 4. POLLUTANTS MONITORING BASED ON RETRIEVED PROFILES

The remote detection of pollutants by FTIR emission spectroscopy requires that the background atmospheric contribution (clean atmosphere) be subtracted from measurement (polluted atmosphere) leading to a background free signature (residual) from which mixing ratios can be estimated. To this end, the spectral radiance of the background atmosphere has to be computed using a radiative transfer model. To be accurate these calculations require many inputs including profiles of pressure, temperature, humidity and several other active molecules in the infrared ( $\text{CO}_2$ ,  $\text{O}_3$ ,  $\text{N}_2\text{O}$ ,  $\text{CH}_4$ ,  $\text{CO}$ ,  $\text{O}_2$  and  $\text{N}_2$ ). Temperature and humidity profiles are highly variable in time and location and are usually supplied from coincident radiosonde measurements while other profiles may be safely estimated using the AFGL atmospheric constituent compilation. Consequently, the accuracy of pollutants monitoring by FTIR emission spectroscopy is often limited by the availability of supporting radiosonde. As a first step in evaluating the potential of our retrieval method in the context of pollutants monitoring, a series of radiance calculations has been performed using retrieved and radiosonde profiles<sup>11</sup>. The main objective was to estimate the spectral residual errors introduced by the use of retrieved profiles.

Figure 4 shows typical spectral residuals corresponding to the measurements performed in August 94 (see Fig. 1). The calculated radiances of the background atmosphere (free of pollutants) were generated with FASCOD3 using radiosondes and retrieved profiles reported in Fig. 2 and the midlatitude summer profiles for other constituents. It is important to note that for radiance calculations corresponding to radiosondes it appeared more reliable to use corrected profiles (dotted curves in Fig. 2a) to compensate for the fact that radiosonde and DBIS measurements were not perfectly coincident in time and direction. It can be seen from Fig. 4a that the spectral residual derived from retrieved profiles compare quite well to those derived from radiosonde profiles. The bottom curve of the graph represents the error of the spectral residual. Overall a 8 % RMS error in residuals may be expected when using profiles retrieved with the minimum information type inversion (section 2).

Another aspect of results depicted in Fig. 4b is the shape of the spectral residual curve. From a theoretical point of view this curve should represent the pure background free signature of pollutants. In practice, the background atmosphere removal is limited. Most of the high frequency structure of the spectral residuals may be attributed to slight errors due to  $\text{H}_2\text{O}$  absorption line parameters used in radiance calculations. In the spectral region from  $820$  to  $950\text{ cm}^{-1}$  the low frequency content of the spectral residual is mainly due to CFCs. The bottom curve of Fig. 4b reproduces the absorption spectrum of CFC-11 and CFC-12 extracted from the HITRAN compilation<sup>12</sup>. There is a good match between CFCs

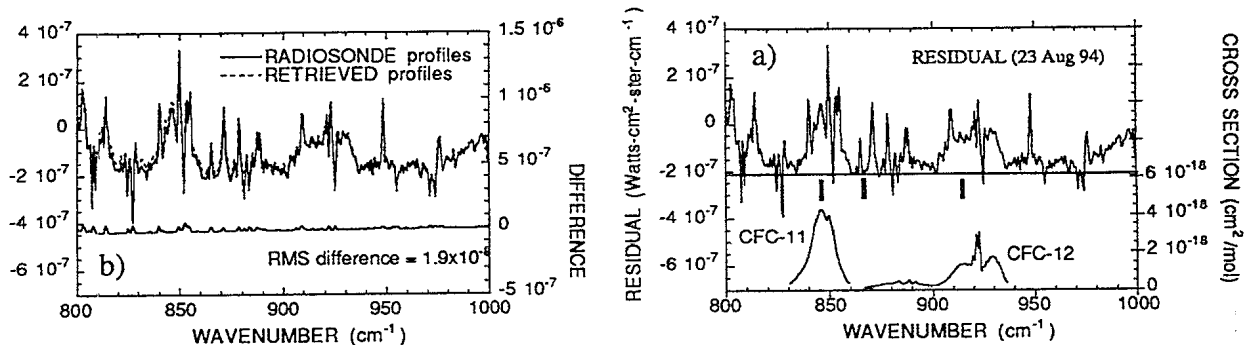


Figure 4: a) Spectral residuals computed with radiosonde temperature and water vapor profiles compared to the residuals obtained using retrieved profiles (bottom curve is the difference). b) Spectral radiance residual (measured minus calculated radiances) compared to absorption cross sections of CFC-11 and CFC-12 (bottom curve: right scale)

and spectral residual curves. The negative offset appearing in the residual curves may have two causes: Experimental errors related to the calibration of the spectrometer and modelling errors due to water vapor continuum parameters intervening in radiance computations.

To illustrate the use of FTIR emission spectroscopy for pollution monitoring the mixing ratios of CFC-11 and CFC-12 has been estimated from the spectral radiance residual (23 August 94) using an approximate relation derived at Ref. 12. Typical errors introduced in mixing ratios by the use of retrieved profiles rather than radiosondes has been estimated to be 1-2 % for CFC-11 and 5-7 % for CFC-12. However the absolute values of mixing ratios found by the approximate relation<sup>12</sup> appears to be higher than current values found in the literature<sup>4</sup> by approximately a factor 1.5.

## 5. CLOUD PARAMETER ESTIMATION

FTIR emission spectroscopy is also a promising technique for the remote sensing of cloud parameters mainly because of its high sensitivity, very wide spectral coverage and spectral resolution. For instance, the work of Ackerman and collaborators<sup>13</sup> on cirrus clouds observed from an airplane with a high resolution interferometer sounder is a convincing example of the great potential of the FTIR technique. The inference of cloud properties from the downwelling spectral radiance requires a full radiative transfer (RT) model which takes into account the cloud scattering and the molecular absorption of atmospheric constituents. With this model it would be possible to infer the apparent temperature and the IR spectral transmittance of a cloud from the match of calculated and measured spectra. Simultaneous retrieval of temperature and humidity profiles together with cloud properties would also be possible. For the time being, existing RT models are not as accurate for cloud scattering as they are for molecular absorption; the inclusion of cloud scattering algorithms in most standard RT models is not fully completed and requires more experimental validations. In this section, a simple method for evaluating the apparent temperature and transmittance of a cloud from the downwelling spectral radiance is proposed.

Figure 5a illustrates the method, where three radiance spectra recorded in the 8 to 12  $\mu\text{m}$  window for different sky conditions are compared: clear, partly transparent cloud and opaque cloud. As seen, the cloud amount tends to decrease the contrast of the ozone emission band near 9.6  $\mu\text{m}$  and the cloud temperature tends to increase the overall emission in the window. To take advantage of this behavior and retain the benefit of a simple estimation procedure, two narrow spectral channels has been selected (vertical bars in Fig. 5a). The choice of this pair is not arbitrary. Channel-1 (1053-1055  $\text{cm}^{-1}$ ) is used to probe the ozone signal and is free of absorption lines. Channel-2 (1093-1094  $\text{cm}^{-1}$ ) depends essentially on the water vapor continuum and is also free of absorption lines. Because the mixing ratio of the ozone peaks at an altitude of 27 km, an important part of the ozone emission (channel-1) occurs above cloud layers. Consequently, the received signal in channel-1 is mainly due to the ozone emission attenuated by the cloud layer. Channel-2 may be seen as a probe for the apparent temperature. Also shown in Fig. 5a, the absorption coefficients of liquid water and ice indicates that water clouds and ice clouds should have approximately the same optical properties in this spectral region. In the 12  $\mu\text{m}$  region, distinct ice and water coefficients would impact differently the resulting radiance.



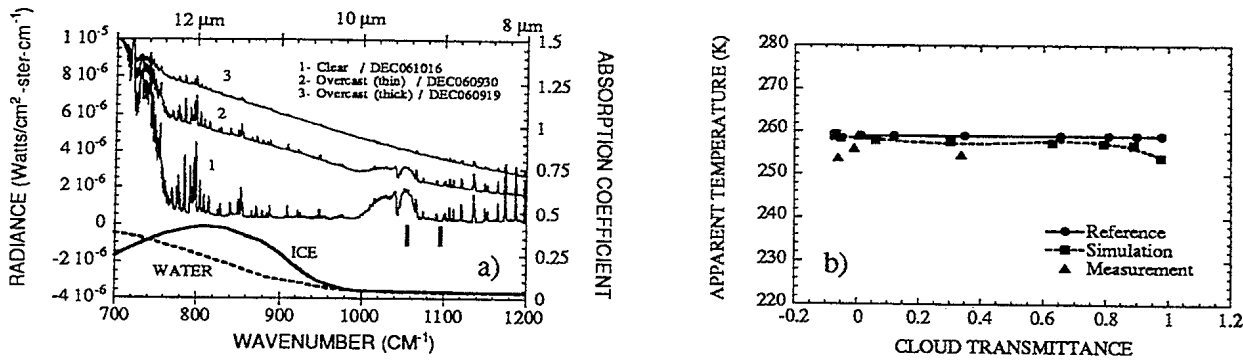


Figure 5: Spectral radiance (a) for different sky conditions compared to the spectral trend of the absorption coefficients of liquid water and ice: Vertical bars correspond to two narrow channels selected for cloud temperature and transmittance evaluation. b) Example of cloud temperature and transmittance evaluation by the method.

To obtain the cloud transmittance at 9.3 μm and its apparent temperature the method requires, first the spectral radiance measurements of the cloudy sky, second the measurement of lidar returns to estimate the cloud height and thickness, third an estimate of temperature and humidity profiles, and finally the measurement of a clear sky radiance to characterize the type of atmosphere which depends on the season and the geographical location. In the case of a broken cloud, the clear sky measurement may be performed directly by selecting a cloud free line of sight near the line of sight of the target cloud. In this case the temperature and humidity profiles may also be obtain by inversion of the clear sky radiance.

In the following, the equations of the method are developed. For a plane-parallel atmosphere in local thermodynamic equilibrium with no scattering, the downwelling spectral radiance  $R(\nu)$  may be expressed in terms of three components

$$R(\nu) = U_{L+1}(\nu) + \epsilon_L(\nu) \tau_L(\nu) + D_L(\nu) \tag{3}$$

where  $L$  is an arbitrary level,  $U_{L+1}(\nu)$  corresponds to the radiance contribution measured at the ground from the atmosphere above level  $L+1$ ,  $\tau_L$  is the transmittance from level  $L$  to the ground,  $\epsilon_L(\nu)$  is defined as the spectral emission of layer  $L$  and  $D_{L+1}(\nu)$  corresponds to the radiance of the atmosphere below level  $L$ . Similarly, the downwelling radiance  $R'(\nu)$  of an atmosphere containing a cloud layer at level  $L$  is given by

$$R'(\nu) = U_{L+1}(\nu) \tau^c + B(\nu) (1-\tau^c) \tau_L(\nu) + \epsilon_L(\nu) \tau_L(\nu) + D_L(\nu) \tag{4}$$

where  $\tau^c$  is defined as the transmittance of the cloud layer,  $(1-\tau^c)B(\nu)$  is the associated gray body radiance of the cloud and  $B(\nu)$  is the Planck equation relating the cloud emission to its apparent temperature. In eq.4 it is assumed that the emission of the cloud-molecule composite layer  $L$  is well approximated by the sum of the two individual emission components (cloud and molecules). Inserting the clear sky radiance eq. 3 into eq. 4 for the two probing channels,  $\nu_a$  (1053  $\text{cm}^{-1}$ ) and  $\nu_b$  (1095  $\text{cm}^{-1}$ ) and assuming that  $\tau^c$  is the same for the two channels yields the system of equations

$$R'(\nu_a) = R(\nu_a) - (1-\tau^c) U_{L+1}(\nu_a) + B(\nu_a) (1-\tau^c) \tau_L(\nu_a) \tag{5}$$

$$R'(\nu_b) = R(\nu_b) - (1-\tau^c) U_{L+1}(\nu_b) + B(\nu_b) (1-\tau^c) \tau_L(\nu_b) \tag{6}$$

The two unknowns to be solved are  $\tau^c$  and  $B$ . Other quantities are properly estimated based on previous clear sky radiance recordings, associated radiosonde or inverted profiles and RT model calculations. Because the Plank radiances  $B(\nu_a)$  and  $B(\nu_b)$  associated to the two probing channels are related by a simple expression

$$B(\nu_b) = 1.462 [B(\nu_a)]^{(1.0399)}, \quad (7)$$

eqs. 5 and 6 can be combined to eliminate the unknown transmittance  $\tau^c$  which gives a simple expression for  $B(\nu_a) = B_a$

$$C_1 (B_a)^{1.0399} + C_2 (B_a) + C_3 = 0, \quad (8)$$

where

$$\begin{aligned} C_1 &= 1.462 m \tau_L(\nu_b), \\ C_2 &= -\tau_L(\nu_a), \\ C_3 &= U_{L+1}(\nu_a) - mU_{L+1}(\nu_b). \end{aligned}$$

and

$$m = \frac{R'_a - R_a}{R'_b - R_b}.$$

$B_a$  is found by solving eq. 8 numerically using the Newton method. In this case, the initial solution  $B_a^0$  is found by assuming that  $B_a = B_b$  in eqs.5 and 6. The final solution (one iteration) is given by

$$B_a = B_a^0 - \frac{F(B_a^0)}{F'(B_a^0)}, \quad (9)$$

where

$$\begin{aligned} F(B_a^0) &= C_1 (B_a^0)^{1.0399} + C_2 (B_a^0) + C_3, \\ F'(B_a^0) &= 1.0399 C_1 (B_a^0)^{0.0399} + C_2, \end{aligned}$$

and

$$B_a^0 = \frac{-C_3}{\frac{C_1}{1.462} + C_2}.$$

Knowing  $B_a$ , it is easy to solve analytically for  $\tau^c$  which is given by

$$\tau^c = 1 - \left( \frac{R'_a - R'_b - R_a + R_b}{C_4 - C_5} \right). \quad (10)$$

with

$$C_4 = B_a \tau_L(\nu_a) - B_b \tau_L(\nu_b).$$

and

$$C_5 = U_{L+1}(\nu_a) - U_{L+1}(\nu_b).$$

Equations 8 and 10 summarize the result of the cloud parameters evaluation method. The apparent temperature of the cloud layer is simply found by inverting the Planck radiance solved at eq.8. It depends on the measured radiances of the cloudy sky  $R'_a$  and  $R'_b$ , and the measured radiances of the associated clear sky  $R_a$  and  $R_b$ . The IR transmittance of the cloud at  $9.6 \mu\text{m}$  is estimated by eq. 10 and depends on the Planck radiances of the cloud  $B_a$  and  $B_b$  (found by eq. 8), the measured radiances of the cloudy sky  $R'_a$  and  $R'_b$  and the measured radiances of the associated clear sky  $R_a$  and  $R_b$ . Constants  $C_1, C_2, C_3, C_4, C_5$  are computed based on radiosonde or inverted profiles obtained in a representative clear sky condition.

Preliminary tests of the cloud evaluation method has been performed on a case where coincident spectral radiance, radiosonde and lidar data were recorded. The temperature at ground level was 271 K and the sky was totally covered by a cloud layer of variable opacity. Inspection of the lidar returns indicates a cloud base smoothly defined at an altitude of 1.4 km and a cloud thickness of approximately 0.4 km. At this altitude range (1.4-1.8 km) the radiosonde data exhibit a very weak temperature inversion, averaging around 259 K. This should correspond approximately to the apparent temperature of the cloud since the atmosphere is assumed to be in thermal equilibrium.

A first test of the method was achieved on simulations calculated with a version of the RT model MODTRAN2. For that, meteorological inputs to MODTRAN2 (temperature and humidity) correspond to the radiosonde profiles and the background atmosphere was assumed to be midlatitude winter. Note that for these simulations the multi-scattering option was not utilized. The cirrus cloud model option included in MODTRAN2 was selected because it offers enough flexibility to select the cloud altitude and thickness. To be consistent with the actual measurements, these parameters were fixed at 1.4 km and 0.4 km respectively. In addition to altitude and thickness, the cirrus cloud option allows the adjustment of the cloud IR transmittance through an absorption coefficient defined at visible wavelength. Taking advantage of this capability, several simulated radiances have been generated for different cloud transmittances. These radiance simulations were then used to test eqs. 8 and 10.

Results of this test are assembled in Fig. 5b. The reference curve is defined as the "truth" which correspond to the temperature-transmittance inputs used in MODTRAN2 simulations. For comparison, the apparent temperatures and the cloud layer transmittance ( $9.3 \mu\text{m}$ ) derived from the evaluation method are also shown in Fig. 5b (simulation curve). As seen, the overall agreement between the two curves is good. However the cloud evaluation method slightly underestimate the apparent temperature with a maximum difference of 5 K for the highest transmittance. In addition, there is a variable offset of the transmittance toward negative values. These discrepancies represent the effect of the few assumptions used to establish eqs. 8 and 10, the most important being the approximation concerning the emission of the composite layer (cloud + molecules). This assumption has to be refined in future work. Finally the evaluation method has been tested on experimental spectra and results are reported in Fig. 5b (measurement). In this case, the evaluation method gives the right order of magnitude but again it seems to underestimate the apparent temperature by approximately 4 K on the average. A part of this discrepancy may be attributed to the fact that the actual line of sight of the instrument does not correspond exactly to the radiosonde path; radiosondes were launched 3 km away from the measurement site. Another possible source of discrepancy comes from the fact that radiance measurements contain an additional contribution from the multiply scattered radiation in the cloud while the evaluation method neglects this contribution.

## 6. CONCLUDING REMARKS

A method of remote sensing for the retrieval of temperature and humidity profiles from IR emission spectra has been described and tested on experimental measurements with satisfactory results. This retrieval method has been evaluated in view to support three specific applications. First it has been utilized to evaluate the accuracy of predicting slant path transmittances when remotely sensed profiles of temperature and humidity are used rather than radiosonde profiles. For that, a series of MODTRAN2 transmittance calculations performed with radiosonde profiles have been compared to calculations done with typical retrieved profiles. These comparisons done at different zenith angles and different optical path lengths are very good in all cases with typical transmittance errors of approximately 1 % in the mid IR, 3 % in the far IR and a maximum difference of 4 % near  $12 \mu\text{m}$ . Second to illustrate the possibilities of the remote sensing method as an aid for pollution monitoring, mixing ratios of CFC-11 and CFC-12 have been estimated from experimental spectra using an approximate relation. The agreement between mixing ratios derived with retrieved profiles compare quite well to those derived with the exact radiosonde profiles with typical errors due to uncertainties in temperature and humidity profiles of approximately 7 %. Finally, a first step in the development of a simple method for estimating cloud temperature and transmittance from the downwelling spectral radiance has been reported. Preliminary results of the method are encouraging enough to justify more analyses of actual data. Future work should be oriented to evaluating the impact of multiple scattering on cloud temperature and transmittance determinations.

## 7. ACKNOWLEDGEMENTS

The authors would like to thank Jean-Luc Moncet from AER for the helpful collaboration in the elaboration of the inversion algorithm. We also thank Luc Bissonnette, Gilles Roy and François Nicolas from DREV for many useful suggestions related to this work.

### 8. REFERENCES

1. W. L. Smith et al., "GAPEX: A Ground-Based Atmospheric Profiling Experiment", *Bulletin of the American Meteorological Society*, vol. 71, 310, 1990.
2. J.-M. Thériault, G. P. Anderson, J. H. Chetwynd, E. P. Murphy, V. Turner, M. Cloutier, A. Smith and J. L. Moncet, "Retrieval of Tropospheric Profiles from IR Emission Spectra: Preliminary results with the DBIS", *Conference on High Latitude Optics, European Optical Society / SPIE, Norway*, pp. 10, July 1993.
3. D. Lubin and A.S. Simpson, "The longwave emission signature of urban pollution: Radiometric FTIR measurement", *Geophys. Res. Lett.*, Vol. 21, 37, 1994.
4. W.F.J. Evans and E. Puckrin, "An Observation of the Atmospheric Thermal Emission Spectrum of Trichlorofluoromethane (CFC-11)", *Geophys. Res. Lett.*, Vol. 21, 2381, 1994.
5. G. P. Anderson, S. A. Clough, F. X. Kneizys, E. P. Shettle, J. H. Chetwynd and L. W. Abreu, "FASCOD3 Update", *Proceeding of the 12th Annual Review Conference on Atmospheric Transmission Models, Geophysics Laboratory, Hanscom AFB, MA: 163, 1989.*
6. C. D. Rodgers, "Retrieval of Atmospheric Temperature and Composition from Remote Measurements of Thermal Radiation", *Reviews of Geophysics and Space Physics*, Vol. 14, 609, 1976.
7. J. L. Moncet, Atmospheric and Environmental Reseach, Inc., Cambridge MA, Private communication. 1993.
8. J.-M. Thériault, J. L. Moncet and C. Bradette "Spectral Sensing of IR Atmospheric Parameters", *The European Symposium on Satellite Remote Sensing, Conference on Optics in Atmospheric Propagation and Random Phenomena, European Optical Society / SPIE, Rome, Italy, pp. 12, September 1994.*
9. J.-M. Thériault, J.-L. Moncet, "Inversion of Downwelling Spectral Radiance for Tropospheric Profile Retrievals: Practical Aspects", *Proceeding of the 18th Annual Review Conference on Atmospheric Transmission Models, Geophysics Laboratory, Hanscom AFB, MA: pp. 8, 1995.*
10. G. P. Anderson, J. H. Chetwynd, J.-M. Thériault, P. Acharya, A. Berk, D. C. Robertson, F. X. Kneizys, M. L. Hoke, L.W. Abreu and E.P. Shettle, "MODTRAN2: Suitability for Remote Sensing", *SPIE Proc. 1968 on Atmospheric Propagation and Remote Sensing II, 1993.*
11. J.-M. Thériault, J. Gilbert and C. Bradette "Atmospheric Monitoring with a Ground-based Spectrometer System", *The European Symposium on Optics for Environmental and Public Safety, Conference on Air Toxics and Water Monitors, European Optical Society / SPIE, Fairgrounds Munich, FRG, pp. 11, June 1995.*
12. L. S. Rothman, R. R. Gamache, R. H. Tipping, C. P. Rinsland, M. A. H. Smith, D. Chris Benner, V. Malathy Devi, J.-M. Flaud, C. Camy-Peyret, A. Perrin, A. Goldman, S. T. Massie, L. R. Brown and R. A. Toth, "The HITRAN molecular database: Editions of 1991 and 1992", *J. Quant. Spectrosc. Radiat. Transfer* 48, 469 (1992)
13. S. A. Ackerman, W. L. Smith, J. D. Spinhirne and H. E. Revercomb, "The 27-28 October 1986 FIRE IFO Cirrus Case Study: Spectral Properties of Cirrus Clouds in the 8-12  $\mu\text{m}$  Window", *Mon. Wea. Rev.*, Vol.118, 2377, 1990.



NO. OF COPIES NOMBRE DE COPIES	COPY NO. COPIE N°	INFORMATION SCIENTIST'S INITIALS INITIALES DE L'AGENT D'INFORMATION SCIENTIFIQUE
1	1	BA
AQUISITION ROUTE FOURNI PAR	SPIE	
DATE	20 NOV 96	
DSIS ACCESSION NO. NUMÉRO DSIS	96 - 03522	

DND 1158 (6-87)



**PLEASE RETURN THIS DOCUMENT  
TO THE FOLLOWING ADDRESS:**  
 DIRECTOR  
 SCIENTIFIC INFORMATION SERVICES  
 NATIONAL DEFENCE  
 HEADQUARTERS  
 OTTAWA, ONT. - CANADA K1A 0K2

**PRIÈRE DE RETOURNER CE DOCUMENT  
À L'ADRESSE SUIVANTE:**  
 DIRECTEUR  
 SERVICES D'INFORMATION SCIENTIFIQUES  
 QUARTIER GÉNÉRAL  
 DE LA DÉFENSE NATIONALE  
 OTTAWA, ONT. - CANADA K1A 0K2

#500040